

## Research Article

# Effects of Sulfurization Temperature on Properties of CZTS Films by Vacuum Evaporation and Sulfurization Method

Jie Zhang, Bo Long, Shuying Cheng, and Weibo Zhang

College of Physics and Information Engineering and Institute of Micro-Nano Devices & Solar Cells, Fuzhou University, Fuzhou, Fujian 350108, China

Correspondence should be addressed to Shuying Cheng; [sycheng@fzu.edu.cn](mailto:sycheng@fzu.edu.cn)

Received 19 May 2013; Revised 28 July 2013; Accepted 3 September 2013

Academic Editor: Francesco Bonaccorso

Copyright © 2013 Jie Zhang et al. This is an open access article distributed under the Creative Commons Attribution License, which permits unrestricted use, distribution, and reproduction in any medium, provided the original work is properly cited.

Copper zinc tin sulfur (CZTS) thin films have been extensively studied in recent years for their advantages of low cost, high absorption coefficient ( $\geq 10^4 \text{ cm}^{-1}$ ), appropriate band gap ( $\sim 1.5 \text{ eV}$ ), and nontoxicity. CZTS thin films are promising materials of solar cells like copper indium gallium selenide (CIGS). In this work, CZTS thin films were prepared on glass substrates by vacuum evaporation and sulfurization method. Sn/Cu/ZnS (CZT) precursors were deposited by thermal evaporation and then sulfurized in  $\text{N}_2 + \text{H}_2\text{S}$  atmosphere at temperatures of  $360\text{--}560^\circ\text{C}$  to produce polycrystalline CZTS thin films. It is found that there are some impurity phases in the thin films with the sulfurization temperature less than  $500^\circ\text{C}$ , and the crystallite size of CZTS is quite small. With the further increase of the sulfurization temperature, the obtained thin films exhibit preferred (112) orientation with larger crystallite size and higher density. When the sulfurization temperature is  $500^\circ\text{C}$ , the band gap energy, resistivity, carrier concentration, and mobility of the CZTS thin films are  $1.49 \text{ eV}$ ,  $9.37 \Omega \cdot \text{cm}$ ,  $1.714 \times 10^{17} \text{ cm}^{-3}$ , and  $3.89 \text{ cm}^2/(\text{V} \cdot \text{s})$ , respectively. Therefore, the prepared CZTS thin films are suitable for absorbers of solar cells.

## 1. Introduction

$\text{Cu}_2\text{ZnSnS}_4$  (CZTS) is one of the promising materials for absorbers in thin film solar cells because of its excellent properties for obtaining high efficiency; that is, it has a direct band gap of  $1.51 \text{ eV}$ , very close to optimum band gap of semiconductor used for photovoltaic conversion, and high absorption coefficient ( $\geq 10^4 \text{ cm}^{-1}$ ) [1]. At the same time, it has versatile electrical properties which can suitably be tailored and tuned to the specific need in a given device structure [2–5]. Various methods have been reported to fabricate the CZTS thin films including thermal evaporation [6], sputtering [7], pulsed laser deposition [8], electroplating [9], and hydrazine process [10]. The best efficiencies reported for the pure CZTS solar cells so far have been 8.4% using thermal evaporation and sulfurization [11]. In the study, the CZTS thin films were deposited using a  $150^\circ\text{C}$  vacuum thermal evaporation process and subsequent short (5 min) high-temperature ( $570^\circ\text{C}$ ) atmospheric pressure annealing. Though the efficiency of the solar cells is high, the annealing temperature is a little high and it does not correspond to the designing rule of solar

cells. Therefore, choosing a lower sulfurization temperature to produce CZTS thin films is important.

In our study, we also use thermal evaporation and sulfurization method to produce CZTS thin films. And the effects of the sulfurization temperature on the structural, optical, and electrical properties of the CZTS films are investigated.

## 2. Experiment Details

We fabricated CZTS thin films on floating glasses substrates by vapor-phase sulfurization of thermal and electron-beam (E-B) evaporated precursors. This process consisted of two stages with the sequential evaporation of precursors followed by the vapor-phase sulfurization. We formed the stacked precursors on the substrates by depositing ZnS layers with E-B evaporation, Cu and Sn layers with thermal evaporation orderly. The thickness of each layer was controlled by a film thickness monitor (FTM) on the evaporation equipment. And the thicknesses of the three layers are shown in Table 1 according to the ratio of the constituents. We sulfurized the precursors in an annealing furnace in the atmosphere

TABLE 1: The parameters of the CZT precursors.

Precursors	$d_{\text{Sn}}$ (nm)	$d_{\text{Cu}}$ (nm)	$d_{\text{ZnS}}$ (nm)	$n_{\text{Zn}}/n_{\text{Sn}}$	$n_{\text{Cu}}/(n_{\text{Sn}} + n_{\text{Zn}})$
CZT	145	120	360	1.70	0.704

TABLE 2: Samples at different sulfurization temperatures ( $T_s$ ).

Sample	S11	S12	S13	S14	S15
$T_s$ (°C)	360	400	450	500	560

of  $\text{N}_2 + \text{H}_2\text{S}$  (5%) at temperatures of 360°C–560°C for 2 hours. After sulfurization of the precursors, CZTS thin films were formed. The samples obtained at different sulfurization temperatures are listed in Table 2.

The film thickness was measured by a stylus profiler (TENCOR D100). The crystallinity of the CZTS thin films was ascertained by an X-ray diffractometer with  $\text{Cu K}\alpha$  radiation ( $\lambda = 1.5406 \text{ \AA}$ ). The optical characteristics of the CZTS films were performed by a PerkinElmer Lambda 900 UV/VIS/NIR spectrometer in the wavelength range from 300 nm to 1400 nm at room temperature. The surface morphology was observed by a scanning electron microscope (SEM) (HITACHI S-4800) and an atom force microscope (AFM) (Bruker). A HMS-3000 hall measurement system was used to carry out the carrier concentration, mobility, and resistivity.

### 3. Results and Discussions

**3.1. Structure and Morphology.** Figure 1 shows the XRD patterns of the CZTS films obtained at different sulfurization temperatures. For the films sulfurized at 360°C and 400°C, in the XRD patterns, there exist peaks from CZTS (JCPDS-ICDD no. 00-026-0575). However, there are also several peaks from SnS (JCPDS-ICDD no. 01-073-1859) and CuS (JCPDS-ICDD no. 01-075-2233). When the sulfurization temperature is 450°C, the phases of CuS and SnS disappear but there are some XRD peaks from  $\text{SnS}_2$  (JCPDS-ICDD no. 00-022-0951) besides those from CZTS. When the sulfurization temperature is about 500°C and 560°C, the peaks from secondary phases disappear, and there are only the XRD peaks of CZTS. The result indicates that the CZTS thin films sulfurized below 500°C are a mixture of CZTS polycrystals with SnS, CuS, and  $\text{SnS}_2$  as intermediates, and there is only the CZTS phase with the sulfurization temperature above 500°C. The films have the preferred (112) orientation, and the intensity of peak (112) is increased with the increase of the sulfurization temperature.

The size  $D_{hkl}$  of the crystallites is determined from XRD data by the Scherrer formula:

$$D_{hkl} = \frac{K\lambda}{\beta \cos \theta}, \quad (1)$$

where  $K$  is a constant,  $\beta$  is full width at half maximum (FWHM) in radians,  $\lambda$  is the wavelength of X-ray, and  $\theta$  is the Bragg angle [12]. The  $K$ ,  $\lambda$  values are taken as 0.89, 1.5406 Å for the calculations, respectively.

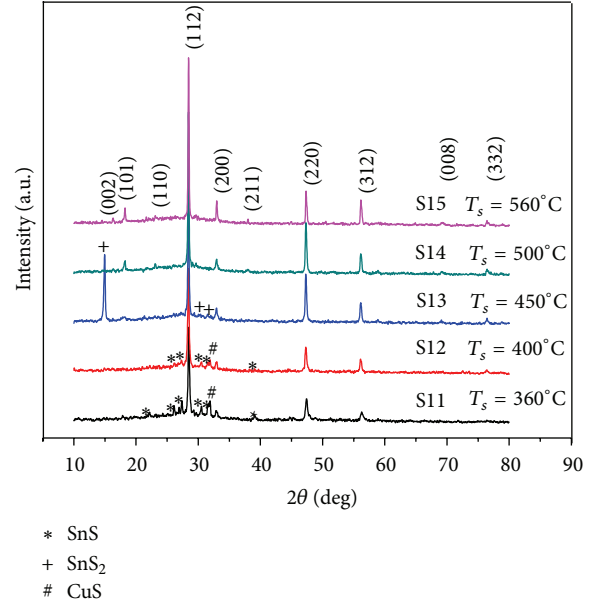


FIGURE 1: The XRD patterns of the CZTS films obtained at different sulfurization temperatures.

TABLE 3: The FWHM values and grain sizes of (112) orientation of the CZTS thin films obtained at different sulfurization temperatures.

Sample	S11	S12	S13	S14	S15
$T_s$ (°C)	360	400	450	500	560
FWHM (°)	0.1968	0.1574	0.1378	0.1200	0.1181
Grain size (nm)	39.92	49.91	57.01	65.47	66.52

TABLE 4: The  $R_{\text{ms}}$  values of the CZTS thin films obtained at different sulfurization temperatures.

Sample	S11	S12	S13	S14	S15
$R_{\text{ms}}$ (nm)	167.2	157.7	116.4	81.0	75.2

Table 3 shows the variation of the grain size from (112) orientation with the sulfurization temperature. With the increase of the sulfurization temperature from 360°C to 560°C, the grain size becomes larger and larger (from 39.92 nm to 66.52 nm).

Figures 2(a)–2(e) show the SEM graphs of the CZTS thin films obtained at different sulfurization temperatures. Figure 2(f) only shows the AFM image of sample S15 for simplification, and Table 4 shows the mean root roughness ( $R_{\text{ms}}$ ) of the CZTS films. We can see that, with the increase of the sulfurization temperature, the grain sizes of the CZTS samples become larger, and the surfaces of the thin films become smoother and denser, which is in agreement with Tables 3 and 4. When the sulfurization temperature is less than 500°C, the CZTS may not be completely synthesized, and thus there are some secondary phases like SnS,  $\text{SnS}_2$ , and CuS as shown in the XRD patterns. When the temperature is 500°C, the film is the most compact. When the temperature is higher than 500°C, the secondary phases disappear and the grain size of the film becomes larger, as seen in Figure 2(e).

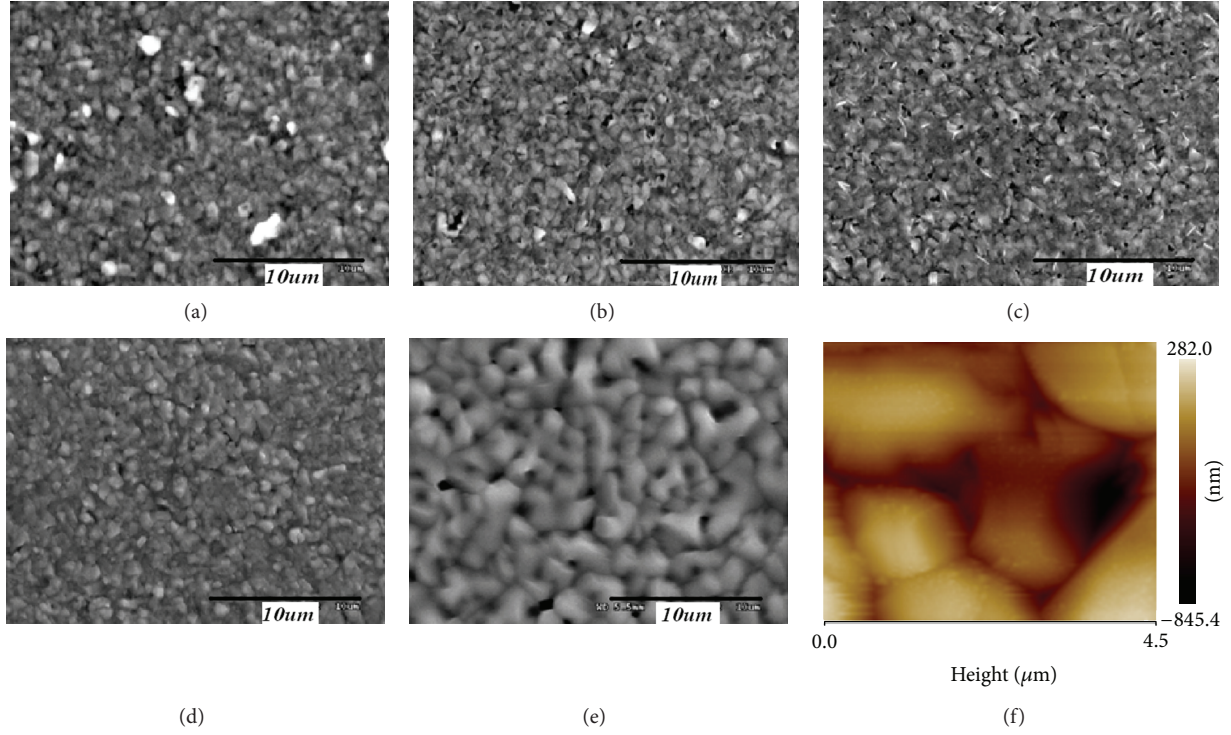


FIGURE 2: The SEM images of the CZTS thin films samples obtained at different sulfurization temperatures: (a) S11 (360°C), (b) S12 (400°C), (c) S13 (450°C), (d) S14 (500°C), (e) S15 (560°C), and (f) AFM image of sample S15.

TABLE 5: The values of  $E_g$  and  $\alpha$  of the CZTS thin films obtained at different sulfurization temperatures.

Sample	$T_s$ (°C)	$E_g$ (eV)	$\lambda_0$ (nm)	$\alpha(\lambda_0)$ (cm <sup>-1</sup> )
S11	360	1.38	898.6	$3.25 \times 10^4$
S12	400	1.40	885.7	$4.43 \times 10^4$
S13	450	1.45	855.2	$2.66 \times 10^4$
S14	500	1.49	832.2	$2.19 \times 10^4$
S15	560	1.57	789.8	$1.18 \times 10^4$

But there are some voids on the surface of the CZTS thin films. It may be due to the loss of Sn at higher sulfurization temperature ( $\geq 500^\circ\text{C}$ ) [13]. It is obvious that the sulfurization temperature has some effects on the phase and crystallinity of the CZTS thin films. Therefore, the suitable sulfurization temperature of CZTS films should be no less than  $500^\circ\text{C}$ .

**3.2. Optical Properties.** Figure 3 shows the optical properties of the CZTS thin films obtained at different sulfurization temperatures. And Table 5 shows the values of  $E_g$  and  $\alpha$  of the CZTS thin films. From Figures 3(a) and 3(b), we can see that, with the decrease of the sulfurization temperature, the transmittance and reflectance of the CZTS films decrease. The reasons may be as follows. One could be due to the surface roughness and the crystallinity. From the SEM graphs and Table 4, it can be seen that, with the decrease of the sulfurization temperature, the surfaces become rougher, resulting in more light scattering. The other one may be due to the secondary phases because the secondary phases are increased

with the decrease of the sulfurization temperature. However, most of these compounds have lower energy gap; thus they can absorb light with longer wavelength. Therefore, in the near-infrared waveband, the lower the sulfurization temperature is, the smaller transmittance and reflectance of the CZTS thin films are.

Figure 3(c) shows the absorbance versus the photon energy ( $h\nu$ ) of the CZTS thin films with different sulfurization temperatures. With the decrease of the sulfurization temperature, the absorbance of the samples in the near-infrared waveband increases. The main reason may be due to the existence of the secondary phases. Figure 3(d) shows that the absorption coefficient ( $\alpha$ ) versus  $h\nu$  of the CZTS thin films. From Figure 3(d), we can see that the absorption edge and the stable  $\alpha$  are increased with the increase of the sulfurization temperature. Figure 3(e) gives that the energy bandgap ( $E_g$ ) of the CZTS thin films becomes larger with the increase of the sulfurization temperature; the detailed data are listed in Table 5. Therefore, the temperature has some effects on the crystallinity, phase, and optical properties of the CZTS thin films. When the sulfurization temperature is below  $500^\circ\text{C}$ , there are some secondary phases, resulting in the worse crystallinity, rougher surface, and smaller  $E_g$ . When the sulfurization temperature is above  $500^\circ\text{C}$ , not only the grain size becomes larger, but also the  $E_g$  is very close to the optimum bandgap of semiconductor used for photovoltaic conversion.

**3.3. Electrical Properties.** Figure 4 shows the electrical properties of the CZTS thin films obtained at different sulfurization temperatures. All the films are of p-type conductivity.

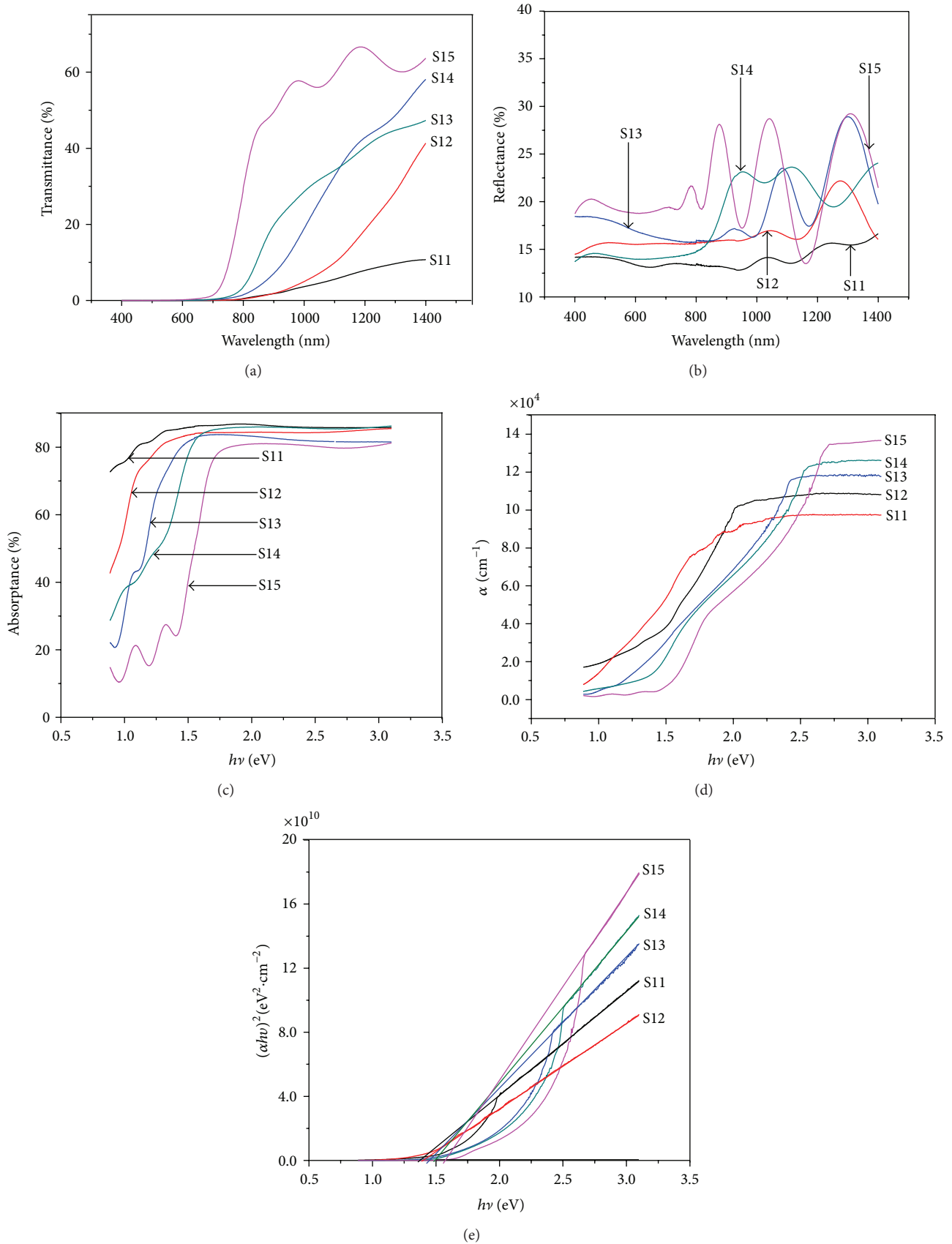


FIGURE 3: The optical properties of the CZTS thin films obtained at different sulfurization temperatures: (a) T, (b) R, (c) absorbance, (d)  $\alpha$ , and (e)  $E_g$ .

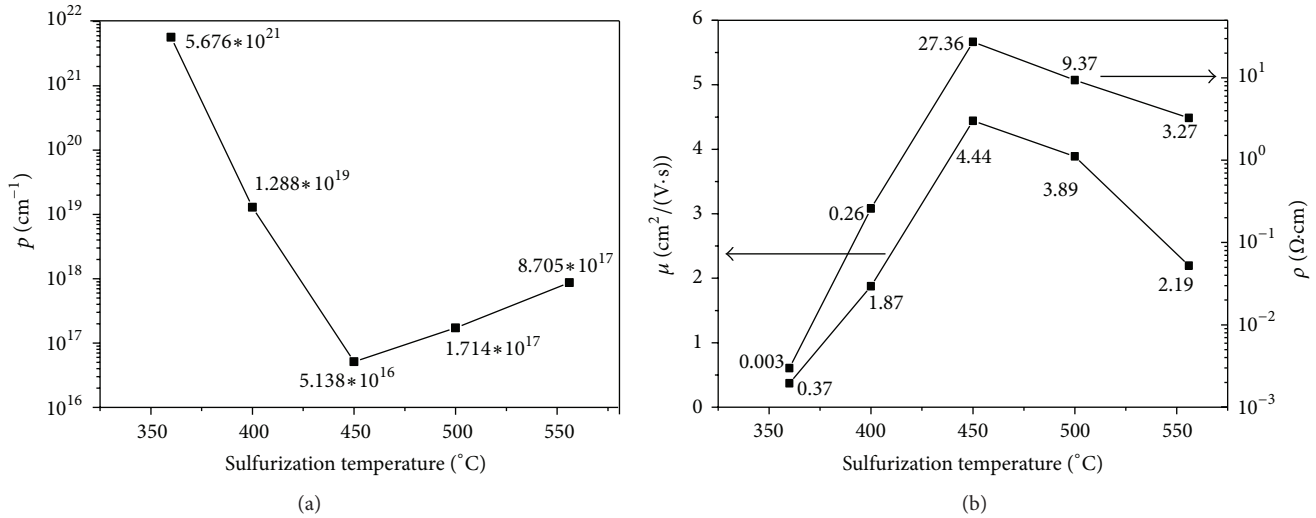


FIGURE 4: The electrical properties of the CZTS thin films obtained at different sulfurization temperatures: (a) carrier concentration ( $p$ ), (b) mobility ( $\mu$ ) and resistivity ( $\rho$ ).

With the increase of the sulfurization temperatures, the carrier concentration is decreased firstly and then increased slowly. But the variation tendency of the mobility and the resistivity are opposite to those of the carrier concentration. Because there are still some binary and ternary compounds in the samples under the low sulfurization temperature, these compounds make the carrier concentration increase. At the same time, they would result in the appearance of some defects and grain boundaries, so the mobility is decreased gradually. With the increase of the sulfurization temperature, the mixed phases are declined. When the temperature is 450°C, we can judge the existence of SnS<sub>2</sub> phase according to the XRD patterns. Whereas SnS<sub>2</sub> is a kind of compound with high resistivity, it may result in the highest resistivity (27.36 Ω·cm) and the lowest carrier concentration (5.138 × 10<sup>16</sup> cm<sup>-3</sup>) of the films. With the increase of the sulfurization temperature, Sn and Zn are lost seriously, resulting in the enlargement of  $n_{\text{Cu}}/(n_{\text{Sn}} + n_{\text{Zn}})$ . Thus, the carrier concentration is increased, and the resistivity is decreased gradually. From the above discussion, we can conclude that the CZTS thin films sulfurized at 500°C have the best electrical properties.

#### 4. Conclusions

The CZTS films were deposited on the glass substrates by thermal and E-B evaporation following sulfurization. With the increase the sulfurization temperature, the crystalline grain size becomes larger, and thereby the crystallinity of the CZTS thin films becomes better. With the increase of the sulfurization temperature, the  $E_g$  of the samples is close to the optimum band gap of the semiconductor used for photovoltaic conversion. At the sulfurization temperature of 500°C, the CZTS thin films have the best electrical properties for PV application.

#### Acknowledgments

This work was supported by the National Nature Sciences Funding of China (61076063) and Fujian Provincial Department of Science & Technology, China (2012J01266).

#### References

- [1] K. Ito and T. Nakazawa, "Electrical and optical properties of stannite-type quaternary semiconductor thin films," *Japanese Journal of Applied Physics*, vol. 27, pp. 2094–2097, 1988.
- [2] D. Park, D. Nam, S. Jung et al., "Optical characterization of Cu<sub>2</sub>ZnSnS<sub>4</sub> grown by thermal co-evaporation," *Thin Solid Films*, vol. 519, no. 21, pp. 7386–7389, 2011.
- [3] C. Shi, G. Shi, Z. Chen, P. Yang, and M. Yao, "Deposition of Cu<sub>2</sub>ZnSnS<sub>4</sub> thin films by vacuum thermal evaporation from single quaternary compound source," *Materials Letters*, vol. 73, pp. 89–91, 2012.
- [4] L. Grenet, S. Bernardi, D. Kohen et al., "Cu<sub>2</sub>ZnSn(S<sub>1-x</sub>Se<sub>x</sub>)<sub>4</sub> based solar cell produced by selenization of vacuum deposited precursors," *Solar Energy Materials and Solar Cells*, vol. 101, pp. 11–14, 2012.
- [5] P. M. P. Salomé, J. Malaquias, P. A. Fernandes et al., "The influence of hydrogen in the incorporation of Zn during the growth of Cu<sub>2</sub>ZnSnS<sub>4</sub> thin films," *Solar Energy Materials and Solar Cells*, vol. 95, no. 12, pp. 3482–3489, 2011.
- [6] F. Biccari, R. Chierchia, M. Valentini, P. Mangiappane et al., "Fabrication of Cu<sub>2</sub>ZnSnS<sub>4</sub> solar cells by sulfurization of evaporated precursors," *Energy Procedia*, vol. 10, pp. 187–191, 2011.
- [7] C. Platzer-Björkman, J. Scragg, H. Flammersberger, T. Kubart, and M. Edoff, "Influence of precursor sulfur content on film formation and compositional changes in Cu<sub>2</sub>ZnSnS<sub>4</sub> films and solar cells," *Solar Energy Materials and Solar Cells*, vol. 98, pp. 110–117, 2012.
- [8] A. V. Moholkar, S. S. Shinde, A. R. Babar et al., "Synthesis and characterization of Cu<sub>2</sub>ZnSnS<sub>4</sub> thin films grown by PLD: solar

- cells," *Journal of Alloys and Compounds*, vol. 509, no. 27, pp. 7439–7446, 2011.
- [9] S. Ahmed, K. B. Reuter, O. Gunawan, L. Guo, L. T. Romankiw, and H. Deligianni, "A high efficiency electrodeposited  $\text{Cu}_2\text{ZnSnS}_4$  solar cell," *Advanced Energy Materials*, vol. 2, no. 2, pp. 253–259, 2012.
- [10] D. A. R. Barkhouse, O. Gunawan, T. Gokmen, T. K. Todorov, and D. B. Mitzi, "Device characteristics of a 10.1% hydrazine-processed  $\text{Cu}_2\text{ZnSn}(\text{Se,S})_4$  solar cell," *Progress in Photovoltaics*, vol. 20, no. 1, pp. 6–11, 2012.
- [11] B. Shin, O. Gunawan, Y. Zhu, N. A. Bojarczuk, S. J. Chey, and S. Guha, "Thin film solar cell with 8.4% power conversion efficiency using an earth-abundant  $\text{Cu}_2\text{ZnSnS}_4$  absorber," *Progress in Photovoltaics*, vol. 21, no. 1, pp. 72–76, 2013.
- [12] P. K. Nair, J. Cardoso, O. Gomez Daza, and M. T. S. Nair, "Polyethersulfone foils as stable transparent substrates for conductive copper sulfide thin film coatings," *Thin Solid Films*, vol. 401, no. 1-2, pp. 243–250, 2001.
- [13] A. Weber, R. Mainz, and H. W. Schock, "On the Sn loss from thin films of the material system Cu-Zn-Sn-S in high vacuum," *Journal of Applied Physics*, vol. 107, no. 1, Article ID 013516, 6 pages, 2010.



**Hindawi**

Submit your manuscripts at  
<http://www.hindawi.com>

